INVESTIGATION OF GENERAL TRENDS IN FAST ROTATING NUCLEI IN THE APPROXIMATION OF THE HARMONIC OSCILLATOR POTENTIAL

By M. Cerkaski and Z. Szymański

Institute for Nuclear Research and University of Warsaw*

(Received July 17, 1978)

Bohr and Mottelson simplification of the Valatin solution for the rotating harmonic oscillator potential is employed to the model analysis of the high angular momentum states in atomic nuclei. The resulting yrast line consists of several trajectories corresponding to fixed nucleonic configurations. Within each trajectory the system tends to acquire oblate, or sometimes prolate shape which is axially symmetric with respect to rotation axis. Dynamical (i.e. resulting from the spectrum) moments of inertia turn out to be of the order of rigid moments for a given nuclear shape. There seems to be no possibility for the existence of yrast traps in the pure harmonic oscillator potential.

1. Introduction

Considerable effort has been devoted within recent few years to the understanding of the properties of fast rotating nuclei [1–3]. One of the possible treatments of nuclear rotation is provided by the liquid drop model of a rotating nucleus [1] which however disregards the role of shell effects. Many other approaches to the analysis of the properties of high angular momentum nuclear states have been attempted on the base of single particle structure of nucleonic motion [4–10]. Calculations of this type employ the concept of the minimisation of nuclear energy at the fixed value of angular momentum. In addition, the minimisation has to be performed with respect to nuclear shape. In most cases the calculations have to rely on the Strutinsky procedure of calculating the shell correction. All these calculations involve rather complicated numerical programs and it seems not too easy to relate various results directly with the original assumptions concerning the input parameters of the model.

On the other hand, an exact solution to the rotating harmonic oscillator potential has been known for many years from the paper by Valatin ([11], see also more recent paper by Ripka et al. [12] as well as [13]). The simple solution resulting from this treatment

* Address: Instytut Badań Jądrowych, Hoża 69, 00-681 Warszawa, Poland.

seems not to have been fully explored in the discussion of the relevant problems in nuclear structure. Obviously, the simplicity of the treatment is achieved on the price of dealing with a very simplified and perhaps not quite realistic potential. Nevertheless, it seems worthwhile to explore the consequences of the rigorous solution offered by Valatin's treatment.

This paper aims at the application of the Valatin solution to the high angular momentum rotation of nuclei. In fact, a rather simplified version of the solution suggested by Bohr and Mottelson [13] is used. In this case the very simple, closed-form expression may be derived for the energy [14]. Moreover, it turns out to be possible to perform explicitly the minimisation of energy with respect to deformation and to classify various configurations by means of the familiar SU(3) group. It has to be emphasized that the precise fit to experimental data in actual nuclei is not the purpose of this paper. It rather aims at the analysis of general trends showing up in fast rotating nuclei that could be derived without any involved computer calculations.

2. *Diagonalisation of the Hamiltonian*

The diagonalisation of the rotating harmonic oscillator (h. o.) has been performed exactly by Valatin [11] (see also [12]) as mentioned before in the introduction. Although a general solution could be used, we shall follow in this paper a simplified version of the model suggested by Bohr and Mottelson [13], based on the approximation valid for not too large nuclear distortions. This approximation enables one to write down many relations in explicit and very transparent form.

We shall assume that single particle motion in the nucleus is described by the triaxial harmonic oscillator. Its Hamiltonian is expressed by the boson creation and annihilation operators $b_\gamma^\dagger(k)$ and $b_\gamma(k)$, respectively. Here, $\gamma = 1, 2, 3$ denotes the spatial component, while index $k = 1, 2, \ldots, A$ is a nucleon label. We have

$$H = \sum_{k=1}^{A} h(k), \tag{2.1}$$

where

$$h(k) = \sum_{\gamma=1}^{A} \hbar\omega_\gamma (b_\gamma^\dagger(k) b_\gamma(k) + \tfrac{1}{2}) \tag{2.2}$$

denotes the one particle Hamiltonian for the k-th nucleon. Quantities $\omega_1, \omega_2, \omega_3$ are the three h. o. frequencies characterising the range and shape of the potential and obeying the volume conservation condition

$$\omega_1 \omega_2 \omega_3 = \overset{0}{\omega}{}^3, \tag{2.3}$$

where $\overset{0}{\omega}$ is a deformation independent constant.

We shall now search for the minimum energy of the system of A particles described by Hamiltonian (2.1) with the subsidiary condition that the expectation value of the

x-component of angular momentum, J_1 is given, and equal to I. This corresponds to the assumption of the nuclear rotation about a fixed axis (x-axis). In order to solve the problem we adopt the cranking Hamiltonian [15]

$$H^\omega = H - \omega\hbar J_1 = \sum_{k=1}^{A} h^\omega(k) \equiv \sum_{k=1}^{A} (h(k) - \omega\hbar j_1(k)), \tag{2.4}$$

where ω plays the role of the Lagrange multiplier. Alternatively, H^ω may be interpreted as the Hamiltonian of the rotating system in the body fixed frame of reference, and ω as the angular velocity of rotation.

Using the appropriately selected phases [16] in the relations of particle coordinates $x_{\gamma k}$ and momenta $p_{\gamma k}$ with the creation and annihilation operators

$$x_{\gamma k} = -i\sqrt{\hbar/(2m\omega_\gamma)}\,(b_\gamma^\dagger(k) - b_\gamma(k)), \qquad p_{\gamma k} = \sqrt{\hbar m\omega_\gamma/2}\,(b_\gamma^\dagger(k) + b_\gamma(k)), \tag{2.5}$$

for $\gamma = 1$ and 3, and

$$x_{2k} = \sqrt{\hbar/(2m\omega_2)}\,(b_2^\dagger(k) + b_2(k), \qquad p_{2k} = i\sqrt{\hbar m\omega_2/2}\,(b_2^\dagger(k) - b_2(k)), \tag{2.6}$$

($k = 1, 2, \ldots, A$) we can obtain all matrix elements (including those of J_1) as real quantities. Indeed, neglecting spin we have

$$J_1 = \sum_{k=1}^{A} j_1(k), \tag{2.7}$$

where

$$j_1(k) = \frac{\omega_2 + \omega_3}{2\sqrt{\omega_2\omega_3}}\,(b_2^\dagger(k)b_3(k) + b_3^\dagger(k)b_2(k)) - \frac{\omega_2 - \omega_3}{2\sqrt{\omega_2\omega_3}}\,(b_2^\dagger(k)b_3^\dagger(k) + b_2(k)b_3(k)). \tag{2.8}$$

The spin part of the angular momentum is omitted throughout this paper.

Although an exact diagonalisation of the cranking Hamiltonian (2.4) is possible for harmonic oscillator, as mentioned before (see [11, 12]), with the inclusion of the complete expression (2.8) for $j_1(k)$, we shall omit the second term in (2.8) as it acts between different major h. o. shells (N, $N \pm 2$) and moreover contains a coefficient of the order of $(\omega_2 - \omega_3)$ which may be small in many physical situations [13]. This assumption restricts somewhat the range of validity of the model as compared to the more exect treatment. On the other hand, as we shall see, the calculations can be greatly simplified in this case, so that many expressions can be written in closed form. As a result of the above assumptions we are left with the diagonalisation of the single particle cranking Hamiltonian

$$h^\omega = \hbar\omega_1(b_1^\dagger b_1 + \tfrac{1}{2}) + \hbar\omega_2(b_2^\dagger b_2 + \tfrac{1}{2}) + \hbar\omega_3(b_3^\dagger b_3 + \tfrac{1}{2}) - \hbar\omega\,\frac{\omega_2 + \omega_3}{2\sqrt{\omega_2\omega_3}}\,(b_2^\dagger b_3 + b_3^\dagger b_2), \tag{2.9}$$

where the index of a k-th particle has been omitted for simplicity.

Diagonalisation of (2.9) can be performed by a standard method of a unitary transformation [13]:

$$b_2^\dagger = b_\alpha^\dagger \cos\varphi + b_\beta^\dagger \sin\varphi, \qquad b_3^\dagger = -b_\alpha^\dagger \sin\varphi + b_\beta^\dagger \cos\varphi. \tag{2.10}$$

Substitution of (2.10) into (2.9) and the appropriate choice of angle φ leads to Hamiltonian h^{ω} expressed in terms of the α and β (normal) modes

$$h^{\omega} = \hbar\omega_1(b_1^{\dagger}b_1+\tfrac{1}{2})+\hbar\omega_{\alpha}(b_{\alpha}^{\dagger}b_{\alpha}+\tfrac{1}{2})+\hbar\omega_{\beta}(b_{\beta}^{\dagger}b_{\beta}+\tfrac{1}{2}). \tag{2.11}$$

The normal frequencies ω_{α} and ω_{β} are given by [13]

$$\omega_{\alpha,\beta} = \tfrac{1}{2}(\omega_2+\omega_3)\pm\tfrac{1}{2}(\omega_2-\omega_3)\sqrt{1+p^2}\,, \tag{2.12}$$

where

$$p = \operatorname{tg}\varphi = \frac{\omega_2+\omega_3}{\omega_2-\omega_3}\frac{\omega}{\sqrt{\omega_2\omega_3}} \approx \frac{2\omega}{\omega_2-\omega_3}\,, \tag{2.13}$$

the last part of equation holding for small (but non zero) values of $(\omega_2-\omega_3)$. The lowest state of the system of A-particles is thus determined by the occupation of A lowest single particle levels. Expressions

$$\Sigma_1 = \sum_{\nu\,\mathrm{occ}}\langle\nu|\,(b_1^{\dagger}b_1+\tfrac{1}{2})\,|\nu\rangle, \qquad \Sigma_{\alpha} = \sum_{\nu\,\mathrm{occ}}\langle\nu|\,(b_{\alpha}^{\dagger}b_{\alpha}+\tfrac{1}{2})\,|\nu\rangle,$$

$$\Sigma_{\beta} = \sum_{\nu\,\mathrm{occ}}\langle\nu|\,(b_{\beta}^{\dagger}b_{\beta}+\tfrac{1}{2})\,|\nu\rangle, \tag{2.14}$$

with $\sum_{\nu\,\mathrm{occ}}$ corresponding to occupancy of A lowest single particle levels determine the total eigenvalue of H^{ω} as

$$E^{\omega} = \hbar\omega_1\Sigma_1+\hbar\omega_{\alpha}\Sigma_{\alpha}+\hbar\omega_{\beta}\Sigma_{\beta}. \tag{2.15}$$

In order to calculate the total energy as the expectation value of H (Eq. (2.1)) in the state that minimizes H^{ω} (Eq. (2.4)) we need furthermore the expression for angular momentum. Employing Eqs. (2.5), (2.6), (2.8) and (2.10) we obtain easily

$$I = \sum_{\nu\,\mathrm{occ}}\langle\nu|j_1|\nu\rangle = (p/\sqrt{1+p^2})\,(\Sigma_{\beta}-\Sigma_{\alpha}). \tag{2.16}$$

This relation together with Eq. (2.13) determines the relation of angular momentum I with angular velocity ω. Solving Eq. (2.16) with respect to p one obtains

$$p = I/\sqrt{I_m^2-I^2}\,, \tag{2.17}$$

where

$$I_m = \Sigma_{\beta}-\Sigma_{\alpha} \tag{2.18}$$

may be interpreted as the maximum angular momentum that can be reached within a given configuration [13].

We can now write down expression for the total energy

$$E = \sum_{\nu\,\mathrm{occ}}\langle\nu|h|\nu\rangle = E^{\omega}+\omega\hbar I. \tag{2.19}$$

Using Eqs. (2.15), (2.17), (2.12) and (2.13) one can rewrite this expression as

$$E = \hbar\omega_1\Sigma_1 + \hbar\omega_2\tilde{\Sigma}_2 + \hbar\omega_3\tilde{\Sigma}_3, \tag{2.20}$$

where

$$\tilde{\Sigma}_{2,3} = \tfrac{1}{2}(\Sigma_\alpha + \Sigma_\beta) \mp \tfrac{1}{2}\sqrt{I_m^2 - I^2}\,. \tag{2.21}$$

Expression (2.20) determines the energy of the system for a given configuration specified by Σ_1, Σ_α and Σ_β for fixed I as well as ω_1, ω_2 and ω_3. However, the shape of nuclear potential characterised by the h. o. frequencies ω_1, ω_2 and ω_3 may also be varied (providing Eq. (2.3) holds) as to minimize energy (2.20). The result of minimization of (2.20) with respect to ω_1, ω_2 and ω_3 with the constraint (2.3) leads to relations

$$\omega_1\Sigma_1 = \omega_2\tilde{\Sigma}_2 = \omega_3\tilde{\Sigma}_3, \tag{2.22}$$

which may be interpreted as the selfconsistency conditions in the rotating potential. The resulting values of ω_1, ω_2 and ω_3 are

$$\omega_\gamma = \overset{0}{\omega}(\Sigma_1\tilde{\Sigma}_2\tilde{\Sigma}_3)^{1/3}/\tilde{\Sigma}_\gamma, \tag{2.23}$$

(with $\gamma = 1, 2, 3$; $\tilde{\Sigma}_1 \equiv \Sigma_1$) determining nuclear deformation for any value of $I \leqslant I_m$. Final expression for the minimized energy is

$$E = 3\hbar\overset{0}{\omega}(\Sigma_1\tilde{\Sigma}_2\tilde{\Sigma}_3)^{1/3} = 3\hbar\overset{0}{\omega}\{\Sigma_1(\Sigma_\alpha\Sigma_\beta + \tfrac{1}{4}I^2)\}^{1/3}. \tag{2.24}$$

This formula, valid for a fixed configuration specified by Σ_1, Σ_α and Σ_β, corresponds to nuclear shape adjusted selfconsistently to minimize energy at each I.

3. Selection of the lowest bands

We have derived expression (2.24) for the energy of a rotating system valid for $0 \leqslant I \leqslant I_m$ and fixed configuration. We shall now search for configurations (Σ_1, Σ_α and Σ_β) that minimize the energy (2.24) at fixed I-value. For this purpose it is convenient to apply the symmetry arguments following from the theory of groups. Let us observe that Hamiltonian H of the system as well as the cranking Hamiltonian H^ω in the approximation (2.9) can be simply expressed by the generators of the harmonic oscillator group U(3). Indeed, the nine operators

$$A_{\gamma\eta} = \sum_{k=1}^{A} b_\gamma^\dagger(k) b_\eta(k) \tag{3.1}$$

(with $\gamma, \eta = 1, 2, 3$; in this section we shall use rather x, y and z) obey the commutation relations

$$[A_{\gamma\eta}, A_{\varepsilon\xi}] = \delta_{\eta\varepsilon}A_{\gamma\xi} - \delta_{\gamma\xi}A_{\varepsilon\eta} \tag{3.2}$$

characteristic for the Lie algebra of the group U(3). Consequently, eigenstates of H^ω can be classified according to labels defining representations of the group U(3), and there

are no matrix elements of H connecting different irreducible representations. Keeping the sum of eigenvalues of diagonal A's fixed:

$$A_{xx}+A_{yy}+A_{zz} = \text{const} \tag{3.3}$$

we may employ the irreducible representations of algebra of the group SU(3) determined by two integers λ, μ (see Ref. [17]; we shall use notation of Ref. [18]). Following a convenient procedure [18] we may label states in the following way

$$|\lambda\mu\varepsilon\Lambda\Lambda_0\rangle, \tag{3.4}$$

where λ, μ determine the representation while ε, $\Lambda(\Lambda+1)$ and Λ_0 are eigenvalues of the operators Q_0, $\vec{\Lambda}^2$ and Λ_0, respectively. They are constructed out of generators $A_{\gamma\eta}$ of U(3) (cf. Eq. (3.1)):

$$Q_0 = 2A_{zz}-A_{xx}-A_{yy}, \tag{3.5}$$

$$\vec{\Lambda}^2 = (A_{xy})^2+(A_{yx})^2+\tfrac{1}{4}(A_{xx}-A_{yy})^2, \tag{3.6}$$

and

$$\Lambda_0 = \tfrac{1}{2}(A_{xx}-A_{yy}). \tag{3.7}$$

The variation of ε, Λ and Λ_0 is determined by

$$\varepsilon = 2\lambda+\mu-3p-3q, \quad \Lambda = \tfrac{1}{2}\mu+\tfrac{1}{2}p-\tfrac{1}{2}q, \quad \Lambda_0 = \tfrac{1}{2}\mu+\tfrac{1}{2}p-\tfrac{1}{2}q-r, \tag{3.8}$$

with

$$0 \leqslant p \leqslant \lambda, \quad 0 \leqslant q \leqslant \mu, \quad 0 \leqslant r \leqslant 2\Lambda; \tag{3.9}$$

(p, q, r — integers). Now, looking at definitions (3.1) of the generators $A_{\gamma\eta}$ and identifying the indices x, y, z with α, β and 1 (of the previous section), respectively, we can write for the many boson state $|\nu\rangle$

$$\varepsilon = 2\Sigma_1-\Sigma_\alpha-\Sigma_\beta, \tag{3.10}$$

$$2\Lambda_0 = \Sigma_\beta-\Sigma_\alpha. \tag{3.11}$$

Furthermore, the sum

$$\Sigma = \Sigma_1+\Sigma_\alpha+\Sigma_\beta \tag{3.12}$$

is fixed as follows from Eq. (3.3). Equations (3.10) to (3.12) can be solved

$$\Sigma_1 = \tfrac{1}{3}\Sigma+\tfrac{1}{3}\varepsilon, \quad \Sigma_\beta = \tfrac{1}{3}\Sigma-\tfrac{1}{6}\varepsilon+\tfrac{1}{2}\nu, \quad \Sigma_\alpha = \tfrac{1}{3}\Sigma-\tfrac{1}{6}\varepsilon-\tfrac{1}{2}\nu, \tag{3.13}$$

(where $\nu = 2\Lambda_0$). Substituting expressions (3.13) into Eq. (2.24) the energy E is obtained as function of Σ, λ, μ, ε and ν for any I. A selection of few best states out of the many states labelled by (Σ, λ, μ, ε, ν) turns out to be possible by the direct minimisation of E

with respect to quantum numbers ε and ν. Detailed calculations can be found in Section (3.4) of Ref. [14]. As a result we obtain three energy bands:

$$E_{\mathrm{L}} = \hbar\overset{0}{\omega}\{(\Sigma-\lambda-2\mu)\,[(\Sigma+2\lambda+\mu)\,(\Sigma-\lambda+\mu)+\tfrac{9}{4}\,I^2]\}^{1/3}, \quad 0 \leqslant I \leqslant \lambda, \tag{3.14}$$

$$E_{\mathrm{M}} = \hbar\overset{0}{\omega}\{(\Sigma-\lambda+\mu)\,[(\Sigma-\lambda-2\mu)\,(\Sigma+2\lambda+\mu)+\tfrac{9}{4}\,I^2]\}^{1/3}, \quad 0 \leqslant I \leqslant \lambda+\mu, \tag{3.15}$$

$$E_{\mathrm{H}} = \hbar\overset{0}{\omega}\{(\Sigma+2\lambda+\mu)\,[(\Sigma-\lambda+\mu)\,(\Sigma-\lambda-2\mu)+\tfrac{9}{4}\,I^2]\}^{1/3}, \quad 0 \leqslant I \leqslant \mu. \tag{3.16}$$

These three bands correspond to the cranking of the nucleus about three principal axes of largest (E_{L} — lowest band), medium (E_{M}) and smallest (E_{H} — highest band) moments of inertia.

In the following, we shall use in our calculation formulae (3.14) to (3.16). However, let us end this section with a short comment on the more general treatment employing the complete Valatin solution. As already mentioned before, the exact treatment of the cranking Hamiltonian H^{ω} with the full expression (2.8) for angular momentum is also possible [11, 12]. In this case transformation (2.10) would have to be replaced by a more general one that involves both creation and annihilation operators

$$\alpha_{\gamma}^{\dagger} = \sum_{\varepsilon}(\lambda_{\gamma\varepsilon}b_{\varepsilon}^{\dagger}+\mu_{\gamma\varepsilon}b_{\varepsilon}), \qquad \alpha_{\gamma} = \sum_{\varepsilon}(\lambda_{\gamma\varepsilon}^{*}b_{\varepsilon}+\mu_{\gamma\varepsilon}b_{\varepsilon}^{\dagger}). \tag{3.17}$$

The existence of term $(b_2^{\dagger}b_3^{\dagger}+b_2b_3)$ in (2.8) leads to an extention of the SU(3) algebra to a noncompact group Sp(3, R) (see Ref. [19]) including all possible products $b^{\dagger}b^{\dagger}$ and bb in addition to $b^{\dagger}b$. The application of transformation (3.16) to Hamiltonian (2.4) with the full expression (2.8) leads again to the three normal modes for the resulting diagonalized form of H^{ω} (see Refs. [11, 12]). One then obtains a new three-dimensional h. o. Hamiltonian expressed in terms of the new generators forming a new U(3) group which is a subgroup of Sp (3, R). The basic vectors forming new irreducible representations of SU(3) could be constructed out of mixtures of the original h. o. states over several major shells. We shall not follow this line in our paper.

4. Search for the yrast configurations

In previous sections we have described the diagonalisation of the cranking Hamiltonian and the selection of the lowest energy rotational band for each representation of the group U(3). In order to complete our procedure we should now give a prescription for the U(3) representation that leads to the lowest energy for given angular momentum I and number of particles A. Since the quantity Σ appearing in Eqs. (3.14) to (3.16) can be found by simple arguments following from the distribution of particles over the h. o. shells (see Eq. (4.6) below) we are left with the search for the quantum numbers λ and μ determining the irreducible representations of SU(3).

The problem can be solved in two steps. If certain distribution of particles over the h. o. shells is known we first have to determine $(\lambda_i\mu_i)$ for each shell "i" separately and then the final irreducible representation $(\lambda\mu)$ is selected out of the outer product of representa-

tions $(\lambda_i \mu_i)$ entering the consideration. We shall illustrate this procedure by examples given in the next section.

In this way, we can reduce our problem to a search for the $(\lambda\mu)$ representation within given h. o. shell. In order to achieve this last goal we employ now two different methods. We shall briefly describe them below and then give examples in next section. First of all, most powerful technique of pletysm [20] can be employed. It is based on the group theoretical determination of what are the SU(3) irreducible representations corresponding to the set of n particles located on a given h. o. shell, N with certain particle symmetry $\{\nu\}$. Here $\{\nu\}$ denotes the particle Young diagram. To each single box in this diagram there corresponds an N-row Young diagram $[N]$ of a system of N h. o. phonons (completely symmetric state). This can be illustrated by the symbolic relation

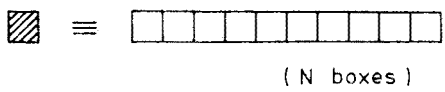

or

$$\{1\} \equiv [N].$$

Here, the shadowed box corresponds to one particle Young diagram, while the N-row diagram (not shadowed) — to N phonons of the h. o. Now, the symmetry $\{\nu\}$ of n particles (in the N-th h. o. shell) will generate some of the phonon Young diagrams that can be found among the states occurring in the outer product of n diagrams of the type $[N]$ each:

$$[N] \times [N] \times \underset{(n \text{ times})}{\cdots} \times [N].$$

The operation of pletysm selects only those representations $(\lambda^{(j)}, \mu^{(j)})$ that correspond to the particle symmetry $\{\nu\}$. This is written down in the following way

$$[N] \otimes \{\nu\} = \sum_j (\lambda^{(j)}, \mu^{(j)}), \tag{4.1}$$

where symbol $\otimes$ denotes the operation of pletysm.

We shall not describe here the details of calculation of various pletysms. They can be found in literature [20, 21]. Instead, in Table I we give the example illustrating the pletysms for one, two, three, and four particles in the $N = 2$ h. o. shell. According to Eq. (4.1) the square bracket [ ] denotes a Young diagram for a phonon state, curly bracket { } — the Young diagram for a particle symmetry and the ordinary bracket ( ) — the $(\lambda\mu)$ (phonon) representation of SU(3) (that could also be expressed as a Young diagram [ ]). If we deal with identical particles of spin $\frac{1}{2}$, only those particle diagrams $\{\nu\}$ are allowed that contain no more than two columns. So, for example, out of those included in Table I the diagrams {3}, {4} and {31} would not be allowed. On the other hand, in the case of protons and neutrons all particle diagrams $\{\nu\}$ with number of columns not exceeding 4 are allowed, as follows from Pauli principle. Now, out of all $(\lambda\mu)$ representations occurring in the pletysm (4.1) the one that leads to lowest energy band should be selected. The selection should be done by a direct check which $(\lambda\mu)$ lead to lowest energies in Eqs. (3.14) to (3.16). However, common experience is that usually the representations with largest possible values of λ and μ are really important.

TABLE I

Pletysms for one, two, three, and four particles in the (sd) shell. Square bracket $[N]$ denotes the Young diagram for phonon state, curly bracket $\{\nu\}$ denotes a diagram for the particle symmetry, and ordinary brackets $(\lambda^{(j)}\mu^{(j)})$ denote the labels for the irreducible SU(3) representations entering the pletysm

$[N]\otimes\{\nu\}$	$\sum_j (\lambda^{(j)}\mu^{(j)})$
$[2]\otimes\{1\}$	(2, 0)
$[2]\otimes\{2\}$	(4, 0), (0, 2)
$[2]\otimes\{11\}$	(2, 1)
$[2]\otimes\{3\}$	(6, 0), (2, 2), (0, 0)
$[2]\otimes\{21\}$	(4, 1), (2, 2), (1, 1)
$[2]\otimes\{111\}$	(3, 1), (0, 3)
$[2]\otimes\{4\}$	(8, 0), (4, 2), (0, 4), (2, 0)
$[2]\otimes\{31\}$	(6, 1), (4, 2), (2, 3), (3, 1), (1, 2), (2, 0)
$[2]\otimes\{22\}$	(4, 2), (0, 4), (3, 1), (2, 0)
$[2]\otimes\{211\}$	(2, 3), (5, 0), (3, 1), (1, 2), (0, 1)
$[2]\otimes\{1111\}$	(1, 2)

Another method of searching for the best $(\lambda\mu)$ representation proposed by Bohr and Mottelson [22] can be based on the analysis in which order various h. o. single particle states are filled in case of no rotation ($I = 0$). It turns out that first as many quanta as it is permitted by the Pauli principle are located in one dimension (say, z). Then, next group of quanta fills in, say, y-direction and finally as few as possible are placed in the remaining direction (say, x). For a given sum

$$\Sigma = \Sigma_x + \Sigma_y + \Sigma_z \tag{4.2}$$

one then obtains Σ_z as large as permitted by the Pauli principle, and Σ_x as small as possible. For larger n and higher shells there may occur however some irregularities [22]. For example, it may turn out more advantageous to locate one particle in the next shell (thus increasing the total value of Σ) gaining in the minimisation of the product by the further increase of Σ_z with respect to Σ_x and Σ_y owing to the relaxation of the Pauli principle. These cases have to be checked individually.

Apart from the above reservations, a simple formula may be worked out for the lowest energy representation corresponding to n nucleons in the N-th h. o. shell. For example in case of even-even system with the same number of neutrons and protons (n divisible by 4) this formula reads

$$\lambda = 2k(k+1)(N-k+1)+2\nu(2N-4k+\nu-1), \qquad \mu = 4\nu(k-\nu+1), \tag{4.3}$$

where k is the largest positive integer that fulfills inequality

$$k(k+1) \leqslant n/2, \tag{4.4}$$

and

$$\nu = [n-2k(k+1)]/4. \tag{4.5}$$

Let us also add that quantity Σ may be calculated directly from the h.o. spectrum

$$\Sigma = (N+\tfrac{3}{2})n + 2\sum_{N'=0}^{N-1}(N'+1)(N'+2)(N'+\tfrac{3}{2}). \tag{4.6}$$

Knowing λ, μ and Σ we may use Eqs. (3.14) to (3.16) in order to deduce Σ_1, Σ_α and Σ_β. For example in the L-band (Eq. (3.14)) we have

$$\Sigma_1 = (\Sigma - \lambda - 2\mu)/3, \tag{4.7}$$

$$\Sigma_\alpha = (\Sigma - \lambda + \mu)/3, \tag{4.8}$$

$$\Sigma_\beta = (\Sigma + 2\lambda + \mu)/3. \tag{4.9}$$

Finally Eq. (2.24) can be used for the energy of the system at arbitrary angular momentum I.

5. *Results and discussion*

Once the representation $(\lambda\mu)$ is found one can calculate the energy of the lowest bands from Eqs. (3.14) to (3.16). It is interesting to note that the dependence is linear in the plot of E^3 versus I^2. All the three bands L, M and H terminate at $I = \lambda$, $\lambda+\mu$ and μ respectively. Beyond these limits one has to search for another representation $(\lambda\mu)$ by shifting some of the particles to higher shells. An example will illustrate best the procedure. Take ^{24}Mg nucleus i.e. a system of 12 neutrons and 12 protons. We can easily see that in the ground state the first 16 nucleons fill in the two closed shells ($N = 0$ and $N = 1$ h.o. shells), while the remaining $n = 8$ nucleons have to populate the (sd)-shell ($N = 2$). For a system of 4 neutrons and 4 protons the best particle symmetry is given by the Young diagram $\{44\}$. In order to find the corresponding SU(3) phonon symmetries we can evaluate the pletysm [18]

$$[2] \otimes \{44\} = (84)+(73)+(46)+(81)+(54)+(62)^2+(35)+(08)+(43)+(51)^2+(24)^2 + (32)+(40)^2+(13)+(02). \tag{5.1}$$

It is easy to see that the lowest energy configuration will be provided by $(\lambda\mu) = (84)$. One can arrive at the same conclusion if formulae (4.3) to (4.6) are used. For $n = 8$ particles in the $N = 2$ shell we obtain

$$k = 1, \quad \nu = 1; \quad \lambda = 8, \quad \mu = 4, \quad \Sigma = 64. \tag{5.2}$$

Now, formulae (4.7) to (4.9) give for the lowest band (L):

$$\Sigma_1 = 16, \quad \Sigma_\alpha = 20, \quad \Sigma_\beta = 28. \tag{5.3}$$

The energies of the three bands L, M and H can now be calculated from Eqs. (3.14) to (3.16). They terminate at $I_m = 8$, 12 and 4, respectively. They are illustrated in Fig. 1 as straight lines in the plot of E^3 versus I^2. In order to calculate states for higher values

of I one has to go beyond the (sd)-shell. For example, shifting one particle to the (fp)-shell ($N = 3$) we obtain $(\lambda\mu) = (83)$ corresponding to the remaining seven nucleons in the (sd)-shell and $(\lambda\mu) = (30)$ corresponding to one nucleon in the (fp)-shell.

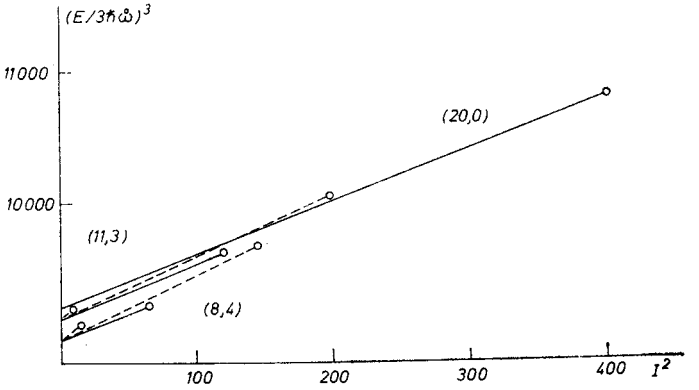

Fig. 1. Dependence of energy E on angular momentum I for the system of 12 protons and 12 neutrons (^{24}Mg). Labels at each band denote the irreducible representations $(\lambda\mu)$ of the SU(3) group. The L-bands are plotted as solid lines, while the M- and H-bands as dashed lines

The product

$$(8, 3) \times (3, 0) = (11, 3) + \ldots \tag{5.4}$$

contains the (11, 3) representation leading to lowest energy band in this region. Using $\Sigma = 65$ one can now calculate the corresponding bands L, M and H leading to $I_m = 11, 14$ and 3, respectively. Similar procedure leads the determination of $\Sigma = 68$ and $(\lambda\mu) = (20, 0)$ for the four particles shifted from (sd)-shell to (fp)-shell (see Fig. 1).

Energy E treated as function of angular momentum I (cf. Eq. (2.24)) increases in the whole range from $I = 0$ to infinity with the inflection point at

$$I = I_{\text{infl}} = \sqrt{12\Sigma_\alpha \Sigma_\beta}\,. \tag{5.5}$$

For $I \ll I_{\text{infl}}$ the curve $E(I)$ looks similar to a parabola. For $I \gg I_{\text{infl}}$ the dependence is weaker: $E \sim I^{2/3}$. However, the physical region of angular momenta usually corresponds to $I \ll I_{\text{infl}}$.

It is interesting to analyze the changes in selfconsistent deformation of the nuclear shape in the rotating nucleus. Formula (2.23) provides us with the values of the harmonic oscillator frequencies ω_1, ω_2 and ω_3 for any value of angular momentum I. Obviously, the condition (2.3) of a constant volume for the potential is fulfilled. It is convenient to introduce the familiar Nilsson ellipsoidal deformation parameters ε, γ (see e.g. Ref. [23]) by the relations

$$\omega_1 = \omega_0(\varepsilon, \gamma)\left(1 + \tfrac{1}{3}\,\varepsilon \cos\gamma + \frac{\varepsilon}{\sqrt{3}} \sin\gamma\right), \tag{5.6}$$

$$\omega_2 = \omega_0(\varepsilon, \gamma)\left(1+\tfrac{1}{3}\,\varepsilon\cos\gamma - \frac{\varepsilon}{\sqrt{3}}\sin\gamma\right), \tag{5.7}$$

$$\omega_3 = \omega_0(\varepsilon, \gamma)\,(1-\tfrac{2}{3}\,\varepsilon\cos\gamma), \tag{5.8}$$

where relation

$$\omega_0(\varepsilon, \gamma) = \overset{0}{\omega}(1-\tfrac{1}{3}\,\varepsilon^2+\tfrac{2}{9}\,\varepsilon^3\cos\gamma-\tfrac{8}{27}\,\varepsilon^3\cos^3\gamma)^{-1/3} \tag{5.9}$$

is obtained by substitution of ω_1, ω_2 and ω_3 given by Eqs. (5.6) to (5.8) into Eq. (2.3). Using Eq. (2.23) we may determine deformation parameters ε and γ for any configuration $(\Sigma_1\Sigma_\alpha\Sigma_\beta)$ and angular momentum I through relation (2.21)

$$\varepsilon = \frac{3(\Sigma_1^{-2}+\tilde{\Sigma}_2^{-2}+\tilde{\Sigma}_3^{-2}-\Sigma_1^{-1}\tilde{\Sigma}_2^{-1}-\tilde{\Sigma}_2^{-1}\tilde{\Sigma}_3^{-1}-\tilde{\Sigma}_3^{-1}\Sigma_1^{-1})^{1/2}}{\Sigma_1^{-1}-\tilde{\Sigma}_2^{-1}+\tilde{\Sigma}_3^{-1}}, \tag{5.10}$$

$$\operatorname{tg}\gamma = \frac{\sqrt{3}\,(\Sigma_1^{-1}-\tilde{\Sigma}_2^{-1})}{\Sigma_1^{-1}+\tilde{\Sigma}_2^{-1}-2\tilde{\Sigma}_3^{-1}}. \tag{5.11}$$

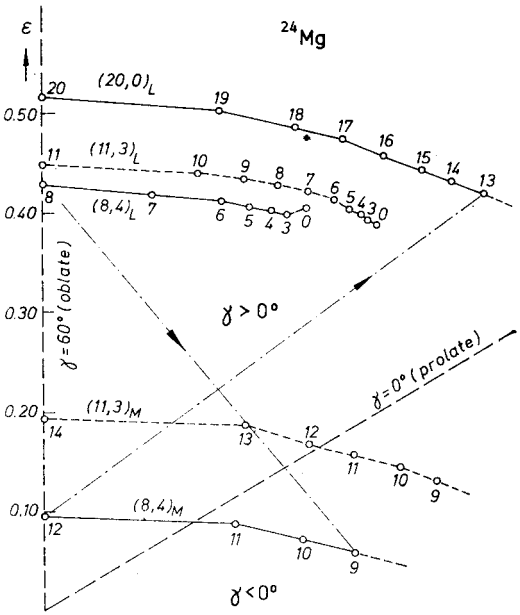

Fig. 2. Spin trajectories in the (ε, γ)-deformation plane for the ^{24}Mg system (cf. Fig. 1). Each band is labelled by $\lambda\mu$ (both L and M-bands). The yrast states are joined with a solid line within a band while various parts of the yrast line are connected with a dot-and-dash line

The spin trajectories corresponding to states marked by dots in the $(\varepsilon\gamma)$ plane are shown for various bands (including the yrast states that are connected by solid line) in Fig. 2. We can see that the ^{24}Mg system which turns out to be triaxial in our model at $I = 0$, approaches the oblate shape $\gamma = 60°$ as $I \to 8$. Similar trends in nuclear deformation in the rotating harmonic oscillator system have been concluded by Neergaard et al. [6].

The conclusion is based on the complete Valatin solution [11]. However the discussion in Ref. [6] is limited to eigenvalue E^{ω} ("the Routhian", cf. our Eq. (2.15)) instead of the energy E (Eq. (2.19)).

Coming back to our example of ^{24}Mg we can see from Fig 2 that for $I > 8$ the system cannot gain any more angular momentum by further increasing its angular velocity, as follows from the oblate shape of the potential. Consequently, further increase of I can be only achieved if the system goes over to another configuration corresponding generally to the triaxial shape at $I \neq 0$. Then the system tends to the oblate limit again following a new trajectory. It has been our numerical experience that at each configuration change the new state corresponds to larger deformation. This could possibly be connected with the analogous trends in the behaviour of the drop of classical liquid that becomes very much elongated at certain angular velocity. However, our model may perhaps be not good enough to describe very deformed shapes as a result of the omission of part of the angular momentum (see Eq. (2.8)). We have seen in the example of ^{24}Mg (Fig. 2) that the system tends to acquire oblate shape with respect to rotation axis ($\gamma = 60°$) within each nucleonic configuration in the L and M bands. This tendency seems to follow as a rule in case of L bands. The situation seems to be more intricate for the M and H bands (cf. Eqs (3.15) and (3.16)). These bands correspond to rotation of the nucleus about the principal axes that are not axes of the largest moment of inertia. In the classical system such rotation never comes to the yrast line as there is always more economic for the system to rotate about the L-axis. However, in the quantal system such a case is possible as first suggested by Neergaard et al. [5, 6] (see also [7]). This can also show up in the rotating harmonic oscillator potential. For example, we have seen (Fig. 1) that in the spin range between 9 and 12 the M-band of the $(\lambda\mu) = (8, 4)$ configuration is the lowest one in the system of 12 neutrons and 12 protons (^{24}Mg). The M trajectory is shown in Fig. 2. One can show generally that for $\lambda > \mu$ the trajectory corresponding to the M band starts in some point $(\varepsilon_0\gamma_0)$ in sector II (i.e. for $-60° \leqslant \gamma \leqslant 0°$, see Fig. 3) and is directed towards sector I ($0 \leqslant \gamma \leqslant 60°$), reaching finally the oblate axis ($\gamma = 60°$) coinciding with the rotation axis. However, for configurations characterised by $\lambda < \mu$ the trajectory looks different: it starts in sector II, but then it extends toward sector III (see Fig. 3) corresponding to the nucleus becoming more and more prolate with the symmetry axis coinciding finally with the prolate rotation axis ($\gamma = 120°$). Configurations of this type seem also to be of interest in case of real nuclei. Finally, for the H-band (which however never becomes yrast) the starting point of the trajectory lies always in sector III and extends toward the prolate axis of symmetry ($\gamma = -120°$). This is also illustrated in Fig. 3.

Another conclusion that seems to follow in our model is connected with the possibility of the existence of yrast traps, that require local minima in the yrast line in the oblate region. The results of this calculation show that the energy is a monotonously increasing function of I. Moreover, there exists in most cases a triaxial state between two oblate ones. This is connected with the fact that each band ends at $I = I_m$ with the oblate shape ($\gamma = 60°$) and the next value of angular momentum corresponds usually to the intermediate states in a new band which are of the triaxial shape. Moreover, the energies of those states appear to lie always on the increasing curve, so that no traps are likely to occur. One can

conclude that the possible existence of the yrast traps in nuclei is perhaps intimately connected with the deviations of the actual nuclear potential from the pure h.o. type (described for example by the $\vec{l} \cdot \vec{s}$ and $\vec{l}^2$ terms in the Nilsson potential). The above argument does

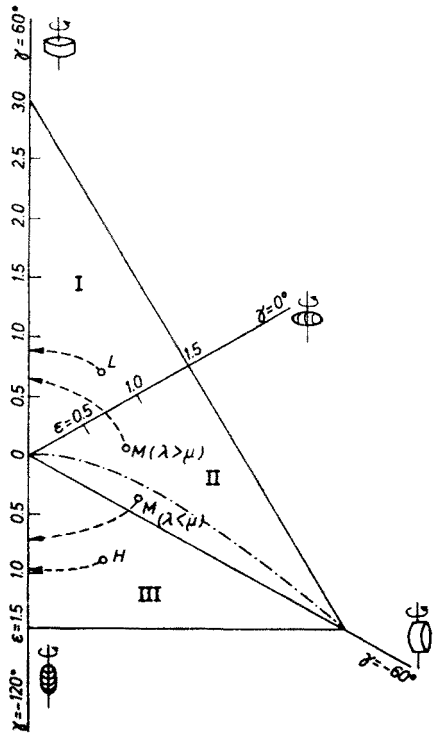

Fig. 3. Schematic plot of the deformation plane (ε, γ). Various possible spin trajectories are indicated with dashed lines. Solid lines mark the border lines between sector I ($0° < \gamma < 60°$), II ($-60° < \gamma < 0°$) and III ($-120° < \gamma < -60°$), as well as the border lines of maximum possible distortions. The dot-and-dash line divides sector II into two regions: ($\lambda > \mu$) abd ($\lambda < \mu$)

not exclude, of course, the possibility for the existence of the high spin isomers emerging from some retardations in the electromagnetic decays.

Let us finally discuss the rotational moments of inertia resulting in our model. Using Eq. (2.24) we obtain

$$\omega = \frac{1}{\hbar}\frac{dE}{dI} = \frac{\overset{0}{\omega}\Sigma_1 I}{2\{\Sigma_1(\Sigma_\alpha\Sigma_\beta + \frac{1}{4}I^2)\}^{2/3}} \tag{5.12}$$

for the angular velocity of rotation, and

$$\mathcal{I}_{\text{dyn}} = \frac{\hbar^2}{2}\left(\frac{dE}{dI^2}\right)^{-1} = \frac{\hbar I}{\omega} = \frac{2\{\Sigma_1(\Sigma_\alpha\Sigma_\beta + \frac{1}{4}I^2)\}^{2/3}}{\Sigma_1} - \overset{0}{(\hbar/\omega)} \tag{5.13}$$

The value of $\mathscr{I}_{\text{dyn}}$ is close to that of the static rigid-body moment of inertia, $\mathscr{I}_{\text{stat}}$ calculated from the expression

$$\mathscr{I}_{\text{stat}} = m \sum_{\nu \text{ occ}} \langle \nu | (y^2 + z^2) | \nu \rangle, \tag{5.14}$$

where the summation runs over all the occupied single particle states (corresponding to normal modes α, β of the transformed Hamiltonian (2.11)). After a straightforward calculation employing Eqs. (2.10) to (2.12) as well as (2.5) and (2.6) we obtain

$$\mathscr{I}_{\text{stat}} = \frac{\Sigma_\alpha^2 + \Sigma_\beta^2 - \frac{1}{2} I^2}{\{\Sigma_1(\Sigma_\alpha \Sigma_\beta + \frac{1}{4} I^2)\}^{1/3}} \overset{0}{(\hbar/\omega)}. \tag{5.15}$$

It is interesting to note that at $I = 0$ we always have $\mathscr{I}_{\text{dyn}} < \mathscr{I}_{\text{stat}}$ (unless $\Sigma_\alpha = \Sigma_\beta$). When I increases from 0 to I_m, $\mathscr{I}_{\text{dyn}}$ increases, while $\mathscr{I}_{\text{stat}}$ decreases approaching common value

$$\mathscr{I} = \frac{(\Sigma_\alpha + \Sigma_\beta)^{4/3}}{(2\Sigma_1)^{1/3}} \overset{0}{(\hbar/\omega)} \tag{5.16}$$

at the end of the band. The changes in $\mathscr{I}_{\text{stat}}$ come only from the changes in nuclear deformation. In fact, $\mathscr{I}_{\text{dyn}}$ and $\mathscr{I}_{\text{stat}}$ do not differ very much even for $I = 0$. For example in the ground band in ^{24}Mg we have

$$\frac{\mathscr{I}_{\text{dyn}}}{\mathscr{I}_{\text{stat}}} = \frac{2\Sigma_\alpha \Sigma_\beta}{\Sigma_\alpha^2 + \Sigma_\beta^2} = \frac{2 \cdot 20 \cdot 28}{20^2 + 28^2} = 0.95.$$

The above discrepancy between $\mathscr{I}_{\text{dyn}}$ and $\mathscr{I}_{\text{stat}}$ may be caused by the omission of the second term from Eq. (2.8) in the cranking Hamiltonian (2.9).

One has also to bear in mind that the above considerations are valid only for a given configuration. When the system changes its configuration with increasing angular momentum the abrupt discontinuities in energy may be interpreted as the average additional increase in the value of the inertial moment. Fig. 4 illustrates the variation of the dynamical moment of inertia $\mathscr{I}_{\text{dyn}}$ as function of angular momentum I (solid line), as well as that of $\mathscr{I}_{\text{stat}}$ (dashed line). The determination of the nuclear moment of inertia from experimental data on the low lying rotational energy levels leads usually to an appreciably lower value than those determined by Eqs. (5.13) or (5.15). For example in the ^{24}Mg nucleus [24] we have $\mathscr{I}_{\text{exp}}/\mathscr{I}_{\text{dyn}} \sim 0.6$ in the ground state band at $I = 0$. This well known discrepancy has been discussed especially extensively in the case of heavier nuclei. The reduction of the nuclear moment of inertia seems to be caused mostly by the short range nucleon--nucleon correlations. We shall not discuss these effects here, as we are mostly interested in the analysis of the overall trends with particular attention directed towards the behaviour at large angular momenta.

In the above analysis we have not employed the renormalisation of the energy to the liquid drop model by means of the shell correction method. This could be done with no difficulty since the suitable expressions for the average smooth energy and angular momentum have been derived for the rotating harmonic oscillator [25, 26]. We have not used

this procedure however, as we were mostly interested in the behaviour of the system following directly from the single particle potential.

Summarising our conclusions we may observe that the yrast line is in the h.o. model composed of various bands corresponding to fixed configurations. Within each band the nucleus tends to approach the oblate shape with angular momentum reaching a certain value $I = I_m$. However, in some special situations (H-bands, or M-bands with $\lambda < \mu$)

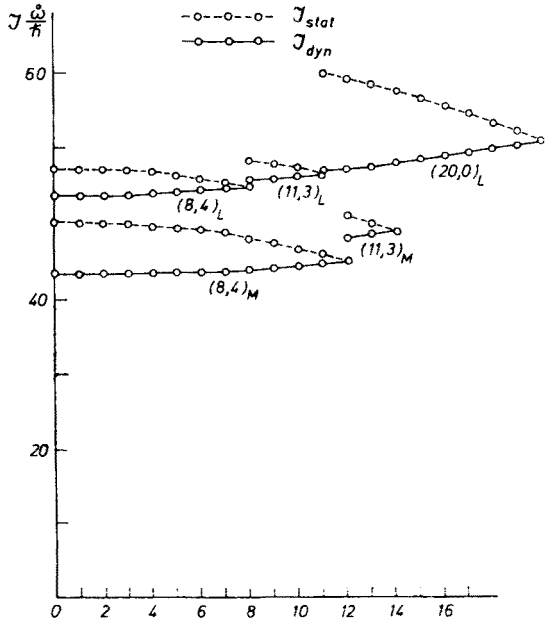

Fig. 4. Dynamic moment of inertia (solid line) as well as the static one (dashed line) plotted for various bands in the ^{24}Mg system as function of angular momentum (cf. Figs 1 and 2)

the end point, $I = I_m$ in the band corresponds to prolate shape. Once the end point of the band is reached the nucleus changes its configuration thus going over to another band which usually corresponds to a more deformed shape. Within each band the cube of energy E is a linear function of the square of the angular momentum I. Dynamical moment of inertia is not equal (although lies very close) to the rigid-body value corresponding to given nuclear shape. At the end of the band the two values coincide. Finally, within the pure harmonic oscillator there seems to be no chance for the existence of the yrast traps since the energy is a monotonous function of angular momentum.

REFERENCES

[1] S. Cohen, F. Plasil, W. J. Świątecki, *Ann. Phys.* (N.Y.) **82**, 557 (1974).
[2] A. Bohr, B. R. Mottelson, *Proc. Nobel Symposium*, Ronneby 1974; see also *Phys. Scr.* **10A**, 13 (1974).
[3] A. Bohr, B. R. Mottelson, invited lecture at Internat. Conf. on Nucl. Structure, Tokyo 1977.
[4] R. Bengtsson, S. E. Larsson, G. Leander, P. Möller, S. G. Nilsson, S. Åberg, Z. Szymański, *Phys. Lett.* **57B**, 301 (1975).

[5] K. Neergaard, V. V. Pashkevich, *Phys. Lett.* **59B**, 218 (1975).
[6] K. Neergaard, V. V. Pashkevich, S. Frauendorf, *Nucl. Phys.* **A262**, 61 (1976).
[7] C. G. Andersson, S. E. Larsson, G. Leander, P. Möller, S. G. Nilsson, I. Ragnarsson, S. Åberg, R. Bengtsson, J. Dudek, B. Nerlo-Pomorska, K. Pomorski, Z. Szymański, *Nucl. Phys.* **A268**, 205 (1976).
[8] A. Faessler, K. R. Sandhya Devi, F. Grümmer, W. K. Schmidt, R. R. Hilton, *Nucl. Phys.* **A256**, 106 (1976).
[9] K. Neergaard, H. Toki, M. Płoszajczak, A. Faessler, *Nucl. Phys.* **A287**, 48 (1977).
[10] K. H. Passler, V. Mosel, *Nucl. Phys.* **A257**, 242 (1976); J. Fleckner, P. G. Zint, V. Mosel, contribution to Int. Workshop on Gross Properties of Nuclei, Hirschegg 1978.
[11] J. G. Valatin, *Proc. Roy. Soc.* **238**, 132 (1956).
[12] G. Ripka, J. P. Blaizot, N. Kassis, invited lecture Internat. Extended Seminar, Trieste 1973, ed. IAEA, Vienna 1975, vol. I, p. 445.
[13] A. Bohr, B. R. Mottelson, *Nuclear Structure*, vol. 2, Benjamin, New York 1975, p. 85 and ff.
[14] Z. Szymański, lectures delivered at École d'Été de Physique Théorique, Les Houches 1977, to be published.
[15] D. R. Inglis, *Phys. Rev.* **96**, 1059 (1954); **97**, 701 (1955); A. Bohr, B. R. Mottelson, *Dan. Mat. Fys. Medd.* **30**, No 1 (1955).
[16] A. Bohr, B. R. Mottelson, see Ref. [13], p. 231 and ff.
[17] J. P. Elliot, *Proc. Roy. Soc.* **245**, 128, 562 (1958).
[18] K. T. Hecht, in *Selected Topics in Nuclear Spectroscopy*, ed. B. J. Verhaar, North-Holland Publ. Co, Amsterdam 1964.
[19] C. G. Andersson, J. Krumlinde, private communication.
[20] D. E. Littlewood, *The Theory of Group Characters and Matrix Representations of Groups*, Clarendon Press, Oxford 1950.
[21] B. G. Wybourne, *Symmetry Principles and Atomic Spectroscopy*, Wiley Interscience.
[22] A. Bohr, B. R. Mottelson, unpublished notes to vol. 3 of *Nuclear Structure*.
[23] S. E. Larsson, G. Leander, Proc. Third IAEA Symposium on Phys. and Chemistry of Fission, Rochester 1973, IAEA, Vienna 1974, paper IAEA-SM-174/06.
[24] P. M. Endt, C. Van Der Leun, *Nucl. Phys.* **A105**, 1 (1967); for more recent data see for ex. A. H. Lumpkin, G. R. Morgan, K. W. Kemper, *Phys. Rev. Lett.* **40**, 104 (1978), and references therein.
[25] M. Brack, B. K. Jennings, *Nucl. Phys.* **A258**, 246 (1976).
[26] I. Hamamoto, unpublished notes, Copenhagen 1974.